Journal of
Materials Chemistry C

Materials for optical, magnetic and electronic devices

Accepted Manuscript

This article can be cited before page numbers have been issued, to do this please use: Y. Nagasaki, H. Nakanotani and C. Adachi, *J. Mater. Chem. C*, 2026, DOI: 10.1039/D5TC04017E.

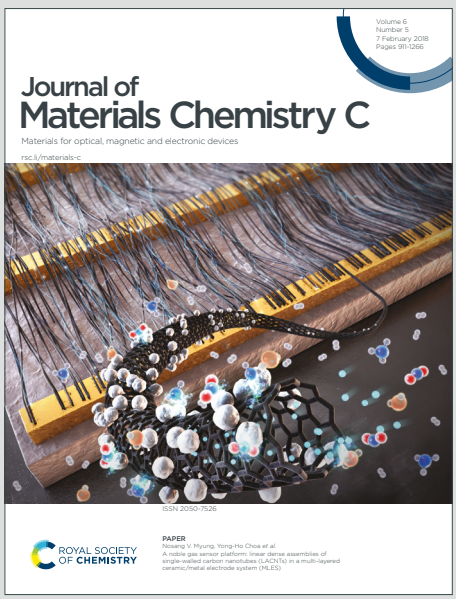

ROYAL SOCIETY OF CHEMISTRY

rsc.li/materials-c

View Article Online
DOI: 10.1039/D5TC04017E

Deuteration Effect on Exciplex Dynamics in Organic Donor–Acceptor Blends

Yuto Nagasaki[1], Hajime Nakanotani[2]*, and Chihaya Adachi[1,3]*

[1]*Center for Organic Photonics and Electronics Research (OPERA), Kyushu University, Motooka, Nishi, Fukuoka 819-0395, Japan*

[2]*Research Institute for Electronic Science, Hokkaido University, N20W10, Kita, Sapporo 001-0020, Japan*

[3]*International Institute for Carbon Neutral Energy Research (WPI-I2CNER), Kyushu University, 744 Motooka, Nishi, Fukuoka 819-0395, Japan*

Abstract

Exciplex systems based on deuterated organic semiconducting molecules provide a promising strategy to enhance the performance of organic light-emitting diodes (OLEDs). Although the enhancement of OLED performance by utilizing a partially deuterated exciplex system has been reported, the impact of deuteration of the organic semiconducting molecule on exciplex dynamics has not been fully characterized. Here, we investigate the impact of deuteration of the electron-donor molecules (**mCP-d_{20}**: 1,3-dicarbazole-benzene-d_{20}) on the exciplex dynamics in the **mCP-d_{20}**:2,4,6-tris[3-(diphenylphosphinyl)phenyl]-1,3,5-triazine (PO-T2T) co-deposited films. Compared to the co-deposited films based on undeuterated mCP, the **mCP-d_{20}**:PO-T2T films exhibited a 1.5-fold increase in photoluminescence quantum yield (PLQY) with prolonged delayed emission lifetime. Temperature-dependent kinetic analyses for electron transition processes revealed that the enhancement of PLQY in the **mCP-d_{20}**:PO-T2T films originates from the suppression of thermally activated nonradiative decay from the excited charge-transfer triplet state by the donor deuteration. Consequently, the OLED based on the deuterated exciplex system demonstrated higher external quantum efficiency than those employing undeuterated donors.

Main Text

Introduction

Organic light-emitting diodes (OLEDs) have garnered significant attention as a key technology for next-generation display applications due to their outstanding features, including ultra-high flexibility, lightweight design, and the potential for low-cost manufacturing. Although OLED displays have been commercialized in various fields, further improvement of OLED performances, such as simultaneously achieving low driving voltage, high external electroluminescence (EL) quantum efficiency (EQE), and stable OLED operation even at ultra-high current densities, is essential for advancing high-performance OLED-based applications, such as ultra-dense micro-OLED displays to support future AR/VR technologies.

According to spin statistics, the electron spin states of the excitons formed *via* charge recombination

events in OLEDs follow the branching ratio of 1:3, yielding the lowest singlet (S_1) and triplet (T_1) excited states, respectively. Since the radiative decay transition from the T_1 state to a ground state (S_0) is a generally spin-forbidden process, to harvest the T_1 energy as bright EL, the use of room-temperature phosphorescent materials containing heavy atoms and/or thermally activated delayed fluorescent (TADF) molecules has been widely investigated [1-4]. In particular, the use of TADF molecules has attracted much attention because the TADF process can serve not only as an emitter but also as a triplet energy harvester in OLEDs, i.e., hyperfluorescence, leading to a highly efficient EL with a narrow EL spectrum [5].

In the TADF process, minimizing the S_1–T_1 energy gap (ΔE_{ST}) is a fundamental key parameter for realizing efficient spin conversion, because the reverse intersystem crossing (RISC) rate constant (k_{RISC}) from the T_1 to the S_1 state is inversely proportional to ΔE_{ST}. To reduce the ΔE_{ST} to a level similar to thermal energy at room temperature, the spatial overlap between the highest occupied molecular orbital (HOMO) and the lowest unoccupied molecular orbital (LUMO) should be carefully minimized. For an ideal TADF process, molecular design strategies frequently employ either intramolecular charge-transfer (CT)-type excited states or intermolecular CT-type excited states. In both cases, when the T_1 energy levels of the electron-donor and electron-acceptor units, *i.e.*, localized T_1 state, lie above the CT-type excited T_1 state, the S_1 and T_1 states of the molecular system should have strong CT character, resulting in the formation of the lowest CT-type excited S_1 and T_1 states (^{1}CT and ^{3}CT) with small ΔE_{ST}. Since the small spatial overlap between the HOMO and LUMO can effectively minimize ΔE_{ST}, exciplexes (intermolecular excited-state complexes) are among the promising molecular systems for efficient TADF [6]. In addition, unlike intramolecular TADF systems, TADF-exciplex is generally composed of two distinct materials, *i.e.*, a hole-transporting material (electron-donor) and an electron-transporting material (electron-acceptor). The donor-acceptor blend not only provides greater molecular tunability but also has the potential to reduce the driving voltage of OLEDs by alleviating charge-injection barriers during operation. In particular, numerous studies have reported the application of TADF-type exciplex as emissive or host layers in OLEDs [6-10].

In addition to the use of efficient TADF-type exciplexes, deuteration of organic molecules has recently attracted significant attention to enhance both EL efficiency and operational stability in OLEDs. Since molecular vibrations, such as C–H stretching modes, are thought to promote nonradiative decay from the excited state to the ground state, lowering their vibrational frequencies by deuteration can be an effective way to suppress nonradiative decay. The improvements in photoluminescence quantum yield (PLQY) resulting from deuteration of emissive molecules have already been reported for several organic molecular systems [11-16]. In addition to the PLQY improvement by deuteration, prolonged OLED operational lifetime has also been reported and is understood to originate from the kinetic isotope effect resulting from hydrogen's mass doubling upon replacement with deuterium [17-21]. Since bond dissociation mediated by radical species or high-energy excited states generated during OLED operation is considered a major cause of device

degradation, reducing the rates of such chemical reactions can improve the operational stability. For example, recent studies have demonstrated that complete substitution of hydrogen with deuterium in deep-blue TADF emitters suppresses high-energy C–H bond vibrations and extends their OLED operational lifetime [15].

A synergistic approach combining both features of TADF-type exciplexes and the deuteration of organic semiconducting molecules should therefore be a promising strategy for the further development of high-performance OLEDs. Although a pioneering work of the deuterated TADF-type exciplex has been reported by W. Yuan et al.[22], the detailed photophysical analysis, such as concentration dependence of deuterated molecule on the TADF-type exciplex dynamics and the rate constants analysis based on the temperature dependence of the exciplex dynamics to unveil the impact of molecular deuteration on the TADF-type exciplex characteristics, has not been fully investigated. Therefore, a comprehensive understanding of the impact of the deuteration on the OLED performances in the TADF-type exciplexes is required. Here, we investigate the impact of the deuteration of the electron-donor molecules on the exciplex emission properties in the electron-donor:acceptor co-deposited films using a 1,3-dicarbazole-benzene (mCP) and its deuterated analogue **mCP-*d*$_{20}$** as the electron-donors together with the electron acceptor molecule 2,4,6-tris[3-(diphenylphosphinyl)phenyl]-1,3,5-triazine (PO-T2T). It was revealed that a nonradiative decay process from the T_1 states was significantly suppressed in the **mCP-*d*$_{20}$**:PO-T2T co-deposited film even at room temperature. The suppression of nonradiative decay was found to become more significant as the fraction of **mCP-*d*$_{20}$** increased in the mCP:PO-T2T co-deposited films, leading to an increase in PLQY from 23 ± 2% (mCP:PO-T2T) to 34 ± 2% (**mCP-*d*$_{20}$**:PO-T2T) with the extended delayed fluorescence lifetime in the **mCP-*d*$_{20}$**:PO-T2T (9:1). Consequently, the maximum external quantum efficiency (EQE) of OLEDs based on the exciplex were improved from 5.5% (mCP:PO-T2T) to 6.4% (**mCP-*d*$_{20}$**:PO-T2T). This study elucidates the photophysical processes of an exciplex incorporating deuterated molecules, providing significant insights into the development of stable, high-efficiency exciplex-based systems.

View Article Online
DOI: 10.1039/D5TC04017E

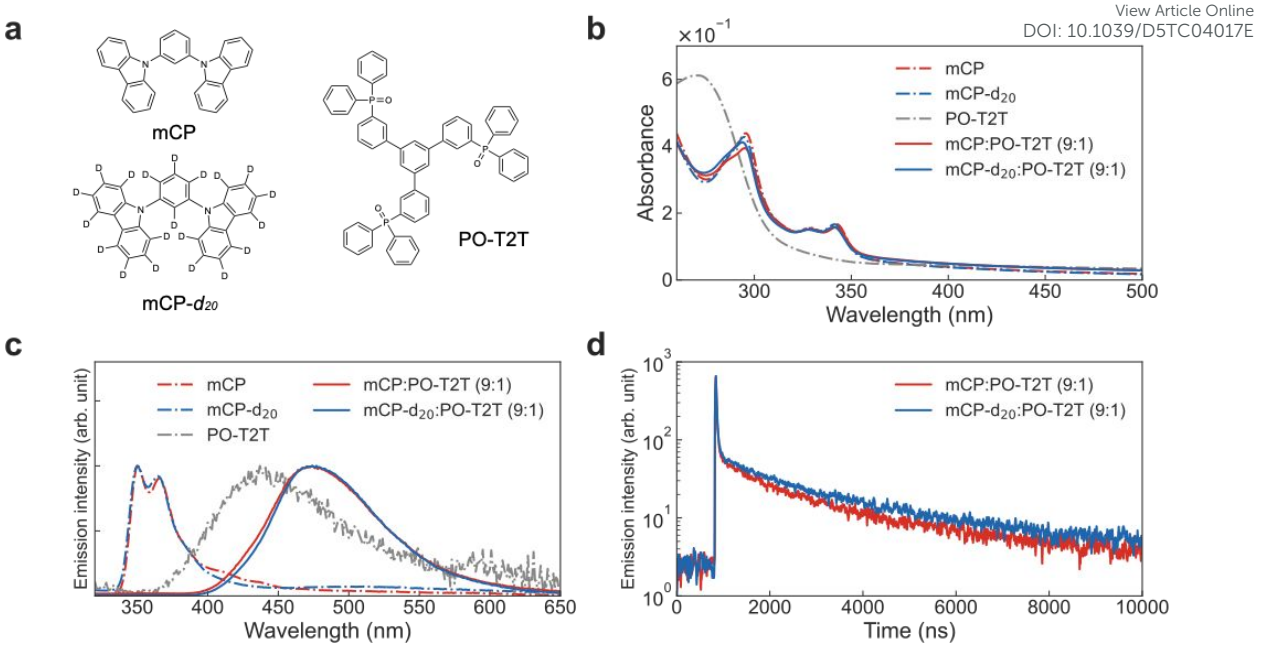

Figure 1: (a) Chemical structures of the molecules used in this study. (b) Steady-state absorption spectra and (c) PL spectra of the mCP, **mCP-*d*$_{20}$**, PO-T2T:PMMA (50wt%), and mCP/**mCP-*d*$_{20}$**:PO-T2T(9:1), respectively. (d) Transient PL profiles of the mCP:PO-T2T, and **mCP-*d*$_{20}$**:**PO-T2T** co-deposited film (9:1) at room temperature.

Results and Discussion

In this study, we used **mCP-*d*$_{20}$** as a deuterated electron donor, which was synthesized according to the previously reported procedure [16]. First, to evaluate the fundamental characteristics of the exciplex formed between mCP (or **mCP-*d*$_{20}$**) and PO-T2T (**Fig. 1a**), UV–visible absorption and photoluminescence (PL) spectra were measured for pure 50 nm-thick deposited films (mCP, **mCP-*d*$_{20}$**, and PO-T2T), and for the mCP (or **mCP-*d*$_{20}$**):PO-T2T co-deposited films (50 nm) with a mixing ratio of 90 mol% mCP (or **mCP-*d*$_{20}$**) and 10 mol% PO-T2T. We also characterize the PL properties of a 50 wt% PO-T2T: polymethyl methacrylate (PMMA) spin-coated film (**Fig. 1b**, and **1c**). The absorption spectra of mCP and **mCP-*d*$_{20}$** films exhibited multiple absorption bands between 250 and 340 nm, while a PO-T2T film showed an absorption band with a peak around 270 nm. In the co-deposited films, only the absorption features attributable to mCP, **mCP-*d*$_{20}$**, and PO-T2T were observed, indicating the absence of CT interactions between mCP/**mCP-*d*$_{20}$** and PO-T2T in the ground state. Although a broad emission band centered around 520 nm was observed in the pure PO-T2T film (**Fig. S1**), it was not observed in the PO-T2T:PMMA film, suggesting that the broad emission originates from excimer formation between neighboring PO-T2T molecules. Furthermore, a distinct emission band centered around 400 nm was observed exclusively in the mCP neat film. Since the emission has a nanosecond time scale, it should be attributed not to room-temperature phosphorescence but to the emission from *J*-aggregated mCP molecules [23]. Interestingly, such emission was not observed in the **mCP-*d*$_{20}$** neat film, likely due to differences in the molecular packing in the **mCP-*d*$_{20}$** film, supported by the difference in the single crystal structure [16]. Although there is no clear CT interaction in the ground state, the PL spectra

of the mCP:PO-T2T and **mCP-*d*$_{20}$**:PO-T2T co-deposited films exhibit a broad and featureless emission band with a peak wavelength of around 480 nm, distinct from the emission of pure mCP, **mCP-*d*$_{20}$**, or PO-T2T films. The emission energy (~2.6 eV) that calculated from the peak emission wavelength well corresponds to the energy difference between the HOMO of mCP/**mCP-*d*$_{20}$** (–6.1 eV) and the LUMO of PO-T2T (–3.5 eV), consistent with the previously reported spectra of mCP:PO-T2T thin films [24], indicating the formation of exciplexes between mCP (or **mCP-*d*$_{20}$**) and PO-T2T molecules. The **mCP-*d*$_{20}$**:PO-T2T co-deposited film completely shares the PL spectrum with that of the mCP:PO-T2T co-deposited film, indicating that the deuteration of mCP did not affect the exciplex emission spectra of the co-deposited films, and similar results were obtained in the mCP (or **mCP-*d*$_{20}$**):PO-T2T co-deposited film with various donor-to-acceptor ratios (**Fig. S2a-b**, and **Table S1**). Collectively, these results demonstrate that deuteration of mCP does not affect the energy levels involved in exciplex emission.

To investigate the impact of deuteration on electron-donor molecules on exciplex dynamics, transient PL profiles (**Figs. 1d** and **S3**) and PLQYs were measured for each co-deposited film. **Table 1** summarizes the emission decay lifetimes and PLQYs of mCP (or **mCP-*d*$_{20}$**):PO-T2T co-deposited films with various donor–acceptor ratios (from 1:9 to 9:1), as well as the radiative decay rate constant from S_1 (k_r^S), nonradiative decay rate constants from S_1 and T_1 (k_{nr}^S, k_{nr}^T), and the rate constants for ISC and RISC (k_{ISC} and k_{RISC}). All rate constants were calculated using a previously reported analytical method [25]. Compared with the

Table 1: Photophysical properties and rate constants for each process of exciplex

Doped film	τ_p (ns)		τ_d (μs)		PLQY (%)		k_r^S (10^6 s^{-1})		k_{nr}^S (10^6 s^{-1})		k_{nr}^T (10^5 s^{-1})		k_{ISC} (10^7 s^{-1})		k_{RISC} (10^6 s^{-1})	
mCP/mCP-d_{20} : PO-T2T	*h*	*d*	*h*	*d*	*h*	*d*	*h*	*d*	*h*	*d*	*h*	*d*	*h*	*d*	*h*	*d*
1 : 9	24	25	3.0	3.2	38 ±3	38 ±4	1.1	1.2	1.8	1.8	2.1	2.0	3.8 ±0.3	3.6 ±0.3	4.6 ±0.1	4.1 ±0.1
3 : 7	25	26	2.9	2.8	37 ±2	42 ±3	1,3	1.8	2.3	2.5	2.2	2.2	3.6 ±0.3	3.4 ±0.3	3.7 ±0.1	3.1 ±0.1
5 : 5	25	24	2.3	2.6	41 ±3	40 ±1	2.4	2.2	3.5	3.3	2.7	2.5	3.5 ±0.3	3.7 ±0.3	2.8 ±0.1	2.9 ±0.1
7 : 3	24	23	2.5	2.5	36 ±1	43 ±3	2.1	2.5	3.8	3.3	2.7	2.4	3.7 ±0.3	3.7 ±0.3	2.8 ±0.1	2.9 ±0.1
9 : 1	21	21	1.7	2.0	23 ±2	34 ±2	2.3	2.8	7.7	5.4	4.8	3.6	4.1 ±0.5	4.1 ±0.4	2.6 ±0.2	2.8 ±0.2

τ_P: Lifetime of the prompt component τ_d: Lifetime of the delayed component
k_r^S: Rate constants for radiative decay from the singlet excited state.
k_{nr}^S: Maximum rate constants for nonradiative decay from the singlet excited state.
k_{nr}^T: Maximum rate constants for nonradiative decay from the triplet excited state.
k_{ISC}: Average rate constants for the ISC process.
k_{RISC}: Average rate constants for the RISC process.

mCP:PO-T2T co-deposited films, the **mCP-*d*$_{20}$**:PO-T2T co-deposited films tended to have prolonged delayed fluorescence lifetimes. Further, the PLQYs of **mCP-*d*$_{20}$**:PO-T2T co-deposited (9:1 and 7:3) films show clear enhancement compared with those of the mCP:PO-T2T co-deposited films. Kinetic analysis revealed that **mCP-*d*$_{20}$** increased the radiative decay rate constant and decreased the nonradiative decay rate constant. This change was particularly pronounced in the co-deposited films with a ratio of 9:1, where k_r^S increased from 2.3×10^6 s^{-1} to 2.8×10^6 s^{-1}, while k_{nr}^S decreased from 7.7×10^6 s^{-1} to 5.4×10^6 s^{-1} and k_{nr}^T decreased from 4.8×10^5 s^{-1} to 3.6×10^5 s^{-1}. Note that the ISC and RISC rate constants remained essentially unchanged in all films, indicating that the deuteration of the donor molecules does not affect the spin-flip processes. Based on these experimental results, deuteration of mCP suppresses nonradiative decay, resulting in longer delayed fluorescence lifetimes and higher PLQYs.

Previous studies have shown that simultaneous deuteration of both host and guest molecules in thin films suppresses molecular vibrations in the solid state, thereby reducing vibration-induced exciton quenching [16]. A similar effect is observed in the exciplex system studied here, where donor deuteration results in comparable suppression of nonradiative deactivation for both singlet and triplet excited states. Furthermore, this trend became more pronounced as the fraction of **mCP-*d*$_{20}$** increased within the co-deposited films. In particular, for the films with 90% **mCP-*d*$_{20}$**, the PLQY increased significantly from 23 ± 2% to 34 ± 2% and the τ_d value simultaneously increased from 1.7 μs to 2.0 μs. Obviously, the emissive species in the co-deposited films were identified as mCP:PO-T2T or **mCP-*d*$_{20}$**:PO-T2T exciplex, and this

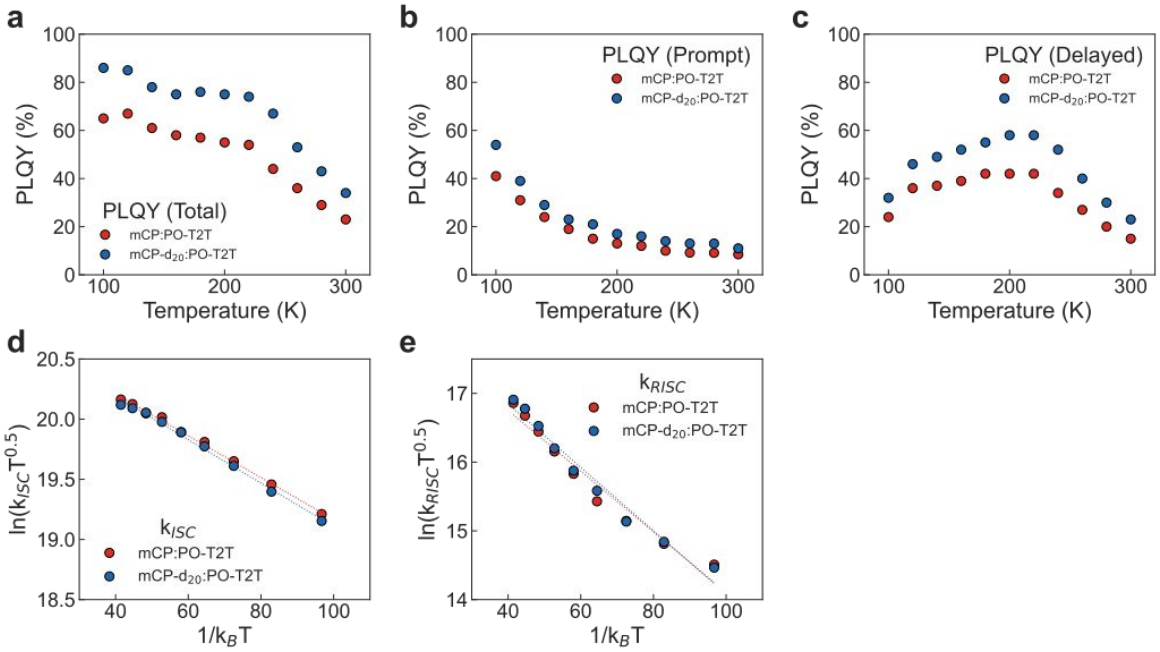

Figure 2: Temperature dependence of PLQY for (a) total emission, (b) prompt emission component, and (c) delayed emission component in the mCP/**mCP-*d*$_{20}$**:PO-T2T(9:1) co-deposition film, respectively. Mercus plot and the activation energy for (d) ISC and (e) RISC rate constant in the mCP/**mCP-*d*$_{20}$**:PO-T2T(9:1), respectively.

assignment should remain consistent for all concentrations. These results therefore highlight that not only the deuteration of emissive species but also that of the surrounding environment is critical for more effective suppression of nonradiative decay. Collectively, these results indicate that increasing the ratio of deuterated donor molecules in the films can effectively suppress vibrational motion and nonradiative decay, thereby enhancing the PLQY of exciplex emission.

To further investigate the effects of donor deuteration on the exciplex emission properties, we examined the temperature dependence of the transient PL characteristics and PLQY in mCP:PO-T2T or **mCP-d_{20}**:PO-T2T films with a donor-to-acceptor ratio of 9:1. The results are summarized in **Figs. 2**, **S4, and Tables S2**, **S3**. In both films, slightly blueshifted steady-state PL spectra were observed as temperature decreased (**Fig. S4**). The delayed emission spectra exhibit a blueshift with decreasing temperature, whereas the prompt emission spectra remain unchanged with varying temperature (**Fig. S5**). This indicates that the blueshifted emission at steady state is due to the delayed emission component's blue shift. The delayed emission has an energy of approximately 2.95 eV (**Figs. S5c** and **5d**), whereas previous studies reported T_1 energies of 3.65 eV for mCP [23] and 3.1 eV for PO-T2T [26], respectively. Therefore, the delayed emission is unlikely to originate from phosphorescence of the T_1 states of the donor, acceptor, or exciplex. Rather, this phenomenon indicated that energy stabilization in both the singlet and triplet excited states is restricted at lower temperatures, leading to changes in the spectra of delayed emission.

Interestingly, the PLQY of the exciplex was increased significantly with decreasing the temperature. The temperature dependence in the total, delayed, and prompt components of the PLQY is summarized in **Fig. 2**. Here, the PLQY values at each temperature were estimated from the integrated PL spectral ratios relative to the absolute PLQY value measured at room temperature. As shown in **Fig. 2a**, the PLQY for total emission in the mCP (or **mCP-d_{20}**):PO-T2T (9:1) film rapidly increases with decreasing temperature (300 ~ 200 K), and then exhibits almost no temperature dependence at the low temperature region (200 ~ 100 K). Further, a similar increase of PLQY in an exciplex system (TCTA:B4PYMPM) has been previously reported [27], but we find that the **mCP-d_{20}**:PO-T2T system exhibits a strong temperature dependence in the PLQY for prompt and delayed emission components, as shown in **Figs. 2b** and **2c**. The PLQY for the prompt component significantly increases with decreasing temperature below 200 K, indicating a temperature-dependent ISC process in the **mCP-d_{20}**:PO-T2T system. Although both systems exhibit similar temperature dependence in the PLQY, the total PLQY in the **mCP-d_{20}**:PO-T2T (9:1) film reached 85% at 100 K, while the mCP:PO-T2T (9:1) film shows low PLQY (63%), highlighting the impact of the deuteration of mCP molecules. **Figure S6** shows the temperature dependence on the PLQY enhancement factor of deuteration obtained by dividing the PLQY of the **mCP-d_{20}**:PO-T2T by that of the mCP:PO-T2T. The enhancement of the PLQY for the delayed component due to donor deuteration was most significant at 300 K and progressively decreased as the temperature decreased. This result indicates that donor deuteration enhances the delayed PLQY at 300 K, where nonradiative decay

is highly active. In contrast, at 100 K, where the nonradiative decay process should naturally be suppressed according to the low temperature, the deuteration effect becomes less significant. Furthermore, the PLQY enhancement of the prompt component showed little temperature dependence. Based on these results, we conclude that the donor deuteration effectively suppresses the nonradiative decay process from the triplet excited state more effectively.

Here, we discuss the ISC and RISC processes in the exciplex system. As discussed above, the PLQY for both prompt and delayed emission components increases with decreasing temperature. To understand these behaviors, the activation energies for both ISC and RISC rate constants were evaluated (**Figs. 2d** and **2e**). Although it is generally believed that an exciplex system has nearly zero ΔE_{ST} because of the significant spatial separation of HOMO and LUMO, we found that both rate constants exhibit an activation energy. For the ISC and RISC processes, an endothermic process with an activation energy of approximately 10 meV and 46 meV, as calculated from the Mercus plot for the k_{ISC} and k_{RISC}, was estimated, respectively. According to the endothermic process, the ISC process should be suppressed at low temperature, leading to the enhancement of the PLQY for the prompt emission component, *i.e.*, radiative decay from the S_1 state. In fact, the PLQY for the prompt component reached 55% at 100 K in the **mCP-*d*$_{20}$**:PO-T2T (9:1) film, which is almost five times higher than that at room temperature. On the other hand, the PLQY for the delayed emission component reaches its maximum around 200 ~ 220 K (PLQY = 58% at 200 K) and tends to decrease with further decrease in temperature (200 ~ 100 K). Generally, the TADF process should be suppressed by decreasing the temperature. However, the **mCP-*d*$_{20}$**:PO-T2T exciplex systems exhibit a clear increase in the PLQY for the delayed component, indicating a significant impact of a vibrationally induced nonradiative decay process on the PLQY in the high-temperature range (300 ~ 200 K). On the other hand, the decrease in the PLQY for the delayed component in the temperature range (200 ~ 100 K) should be considered due to both the suppression of triplet formation (*i.e.*, reduction of the k_{ISC}) and a reduction of the k_{RISC}. In fact, the temperature (200 K) coincides with the starting temperature of the decrease of the PLQY (delayed component) and the starting temperature of the nonlinear increase of the PLQY (for prompt emission).

View Article Online
DOI: 10.1039/D5TC04017E

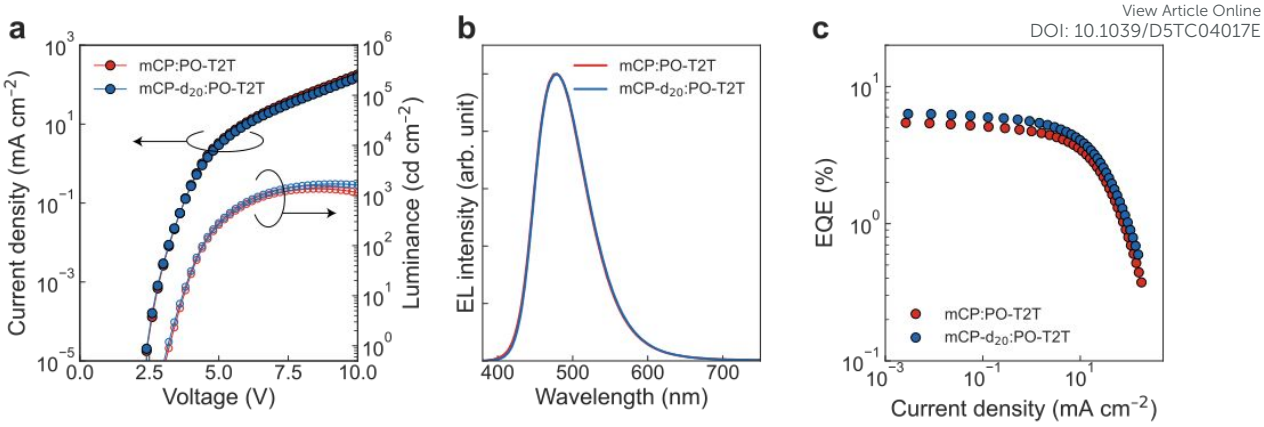

Figure 3: (a) Current-voltage-luminance (*J-V-L*), (b) EL spectra obtained at 8 V, and (c) EQE-*J* characteristics of the tested OLEDs.

Finally, we characterized the EL characteristics of the OLED using the mCP:PO-T2T or **mCP-*d*$_{20}$**:PO-T2T co-deposited layer as the emissive layer to evaluate the impact of donor-molecule deuteration on OLED performance. The donor-to-acceptor ratio in the co-deposited films was fixed at 9:1 because the blend ratio affects PL performance upon deuteration of the donor molecules, and the OLEDs employed the device structure shown in **Fig. S7**. No noticeable change in the current density-voltage characteristics was observed for both types of OLEDs, as shown in **Fig. 3a**. This observation is consistent with the results of the hole-only devices based on mCP and **mCP-*d*$_{20}$** (**Fig. S8b**). Although a previous study has reported that the deuteration of organic materials can provide higher charge transport properties in the solid-state film according to the change of the molecular density [19], the mCP and **mCP-*d*$_{20}$** layers have almost the same hole transport ability in the device structure employed in this study, indicating that donor deuteration does not affect the charge-transporting properties in the OLEDs. In fact, although the film density of the **mCP-*d*$_{20}$** film increased from 1.111 ± 0.056 g/cm³ to 1.163 ± 0.085 g/cm³, which was experimentally obtained using the same method as reported in previous studies [19], this change mainly originated from the substitution with heavier deuterium atoms. In addition, as shown in **Fig. 3b**, no changes in the EL spectrum were observed in either type of OLED, in agreement with the steady-state PL results. Nevertheless, in the **mCP-*d*$_{20}$**:PO-T2T-based OLEDs, the maximum EQE and current efficiency were found to improve clearly (5.5%, 11.6 cd/A for the mCP-based OLED and 6.4%, 14.5 cd/A for the **mCP-*d*$_{20}$**-based OLED) as shown in **Figs. 3c and S9**, and these enhancements in the **mCP-*d*$_{20}$**:PO-T2T-based OLED should be attributed to the enhancement of the PLQY by deuteration of the mCP donor molecules. Although the **mCP-*d*$_{20}$**-based OLED exhibited a higher EQE than the mCP-based OLED, no significant change in operational stability was observed (**Fig. S10**). Note that our results do not mean that the deuteration of organic molecules does not affect the operational stability. The lack of a significant difference in operational stability observed in this study is likely due to the material combination's intrinsic low operational stability (LT50 < 0.3 h for both OLEDs) and/or the limited impact of deuteration on operational stability, since only electron donors were deuterated.

View Article Online
DOI: 10.1039/D5TC04017E

Conclusion

In conclusion, to clarify the impact of deuteration of donor molecules in exciplex systems, the exciplex dynamics in the **mCP-d_{20}**:PO-T2T system were investigated in detail, including the kinetic analysis based on the temperature dependence of the related rate constants. We found that deuteration of donors in the exciplex system significantly reduces nonradiative decay from the triplet excited state, resulting in longer delayed fluorescence lifetimes and higher PLQY than in the mCP:PO-T2T system. Additionally, the deuteration effect becomes more pronounced as the proportion of deuterated donor molecules increases in the films (D:A ratio = 7:3 ~ 9:1), highlighting that the deuteration of surrounding molecules around emissive species is critical in addition to the deuteration of the emissive species. Further, we find that the exciplex systems have activation energies for both ISC and RISC processes (~10 meV and ~46 meV, respectively), leading to an increase in the PLQY of the prompt fluorescent and a decrease in the delayed emission components with decreasing temperature. Further investigations, including the effect of acceptor deuteration, are expected to lead to a deeper understanding and further performance improvement of exciplex-based systems.

Experimental section

Materials and Sample Preparation

1,4,5,8,9,11-Hexaazatriphenylene hexacarbonitrile (**HAT-CN**), **mCP**, **PO-T2T**, and 8-hydroxyquinolinolato-lithium (**Liq**) were purchased from Luminescence Technology Corp. 9-Phenyl-3,6-bis(9-phenyl-9H-carbazol-3-yl)-9H-carbazole (**Tris-PCz**) and **mCP-d_{20}** were synthesized according to previously reported procedures. Organic thin films with a thickness of 50 nm for PL measurements were deposited onto quartz or silicon substrates by thermal evaporation under high vacuum conditions. The deposition was carried out under a vacuum of less than 2.0×10^{-4} Pa. For OLED fabrication, glass substrates patterned with 100 nm-thick indium–tin–oxide (ITO) electrodes were used. The substrates were sequentially cleaned by ultrasonication in neutral detergent, deionized water, acetone, and isopropanol. Residual moisture on the ITO electrodes was removed by boiling isopropanol vapor treatment, followed by drying in nitrogen flow. Subsequently, the substrates were subjected to UV-ozone treatment for 15 min. The cleaned ITO substrates were immediately transferred into the vacuum deposition chamber, where organic and metal layers were successively deposited through appropriate shadow masks. After fabrication, the OLED devices were immediately encapsulated inside a nitrogen-filled glovebox (O_2 < 0.1 ppm, H_2O < 0.1 ppm) using glass covers coated with a moisture-absorbing material (Dynic Co., Ltd.).

Optical Characterization of Organic Thin Films

Steady-state UV/Vis absorption spectra were recorded with a UV–Vis–NIR spectrophotometer (UV-3600 i Plus, Shimadzu Corp.). Steady-state photoluminescence spectra were measured with a spectrofluorometer (FP3600, JASCO Co.) using an excitation wavelength of 300 nm. Photoluminescence quantum yields

View Article Online
DOI: 10.1039/D5TC04017E

(PLQYs) were determined with an absolute PL quantum yield measurement system (Quantaurus-QY, Hamamatsu Photonics) at an excitation wavelength of 300 nm. The PLQY values were obtained as the average of three measurements using independent batches. Transient PL decay curves at room temperature were recorded using a fluorescence lifetime spectrometer (C16361-02, Hamamatsu Photonics). Temperature-dependent PL measurements were conducted using a fluorescence lifetime spectrometer (C16361-01, Hamamatsu Photonics) and a cryostat (CoolSpek, UNISOKU Co., Ltd.). Time-dependent PL spectra were measured by a streak camera system (C4334, Hamamatsu Photonics) using an excitation wavelength of 355 nm.

OLED Characterization

The current density–voltage–luminance (*J–V–L*) characteristics of the OLEDs were evaluated using a source meter (Keithley 2400, Keithley Instruments Inc.) and a calibrated luminance meter (CS-2000A, KONICA MINOLTA). All device measurements were performed in ambient air at room temperature.

Author declaration

Acknowledgement

The authors thank Ms. Yuika Tamura of Kyushu University for preparing the chemicals. This work was partially supported financially by the Japan Society for the Promotion of Science (JSPS) KAKENHI Grant Numbers 23H05406, 23K17367, 23K20039, and 25K01847.

Conflict of Interest

The author declared no conflict of interest.

Author Contribution

The project was conceived and designed by Y.N. and H.N. Y.N. prepared the samples and measured their properties. Y.N. and H.N. analyzed all the data collected in this study. All authors contributed to writing the paper and provided critical comments on the project.

Data Availability

The data supporting the findings of this study are available within the article and its Supporting Information. Additional raw data files are available from the corresponding author upon reasonable request.

Reference

[1] M. A. Baldo, D. F. O'Brien, A. Shoustikov, S. Sibley, M. E. Thompson, S. R. Forrest, *Nature*, **395**, 151-154 (1998).

[2] B. Minaev, G. Baryshnikovb, H. Agrena, Phys. *Chem*. *Chem*. *Phys*., **16**, 1719-1758 (2014).

[3] A. Endo, M. Ogasawara, A. Takahashi, D. Yokoyama, Y. Kato, C. Adachi. *Adv*. *Mater*. **21**, 4802-4806 (2009).

View Article Online
DOI: 10.1039/D5TC04017E

[4] H. Uoyama, K. Goushi, K. Shizu, H. Nomura, C. Adachi. *Nature*, **492**, 234–238 (2012).
[5] C.-Y. Chan, M. Tanaka, Y.-W. Wong, H. Nakanotani, T. Hatakeyama, *Nat*. *Photonics*, **15**, 203–207 (2021).
[6] K. Goushi, K. Yoshida, K. Sato, C. Adachi, *Nature Photon*., **6**, 253-258 (2012).
[7] Y.-S. Park, S. Lee, K.-H. Kim, S.-Y. Kim, J.-H. Lee, J.-J. Kim, *Adv*. *Funct*. *Mater*., **23**, 4914-4920 (2013).
[8] B. Liang, J. Wang, Y. Cui, J. Wei, Y. Wang, *J*. *Mater*. *Chem*. *C*, **8**, 2700-2708 (2020).
[9] J. Sun, H. Ahn, S. Kang, S.-B. Ko, D. Song, H. A. Um, S. Kim, Y. Lee, P. Jeon, S.-H. Hwang, Y. You, C. Chu, S. Kim, *Nat*. *Photonics*, **16**, 212-218 (2022).
[10] H.-T. Cao, P.-F. Hou, W.-J. Yu, Y. Gao, B. Li, Q.-Y. Feng, H. Zhang, S.-S. Wang, Z.-M. Su, L.-H. Xie, *ACS Appl*. *Mater*. *Interfaces*, **15**, 7236-7246 (2023).
[11] R. Englman, J. Jortner, *Mol*. *Phys*. **18**, 145 (1970).
[12] S.-F. Wang, B.-K. Su, X.-Q. Wang, Y.-C. Wei, K.-H. Kuo, C.-H. Wang, S.-H. Liu, L.-S. Liao, W.-Y. Hung, L.-W. Fu, W.-T. Chuang, M. Qin, X. Lu, C. You, Y. Chi, P.-T. Chou, *Nat*. *Photonics*, **16**, 843 (2022).
[13] Y.-C. Wei, K.-H. Kuo, Y. Chi, P.-T. Chou, *Acc*. *Chem*. *Res*. **56**, 689 (2023).
[14] S. Wang, D. Zhou, K. Kuo, C. Wang, C. Hung, J. Yan, L. Liao, W. Hung, Y. Chi, P. Chou, *Angew*. *Chem*., *Int*. *Ed*. **63**, 202317571 (2024).
[15] T. Huang, Q. Wang, H. Zhang, Y. Zhang, G. Zhan, D. Zhang, L. Duan, *Nat*. *Photonics*, **18**, 516-523 (2024).
[16] Q. Yu, Y. Tamura, H. Nakanotani, M. Mamada, C. Adachi, *Adv*. *Opt*. *Mater*., **12**, 2400932 (2024).
[17] P. Wang, F.-F. Wang, Y. Chen, Q. Niu, L, Lu, H.-M. Wang, X.-C. Gao, B. Wei, H.-W. Wu, X. Cai, D.-C. Zou, *J*. *Mater*. *Chem*. *C*. **1**, 4821–4825 (2013).
[18] H. Tsuji, C. Mitsui, E. Nakamura, *Chem. Commun*., **50**, 14870-14872 (2014).
[19] X. Liu, C.-Y. Chan, F. Mathevet, M. Mamada, Y. Tsuchiya, Y.-T. Lee, H. Nakanotani, S. Kobayashi, M. Shiochi, C. Adachi, *Small Sci*., **1**, 2000057 (2021).
[20] W. Li, A. Wu, T. Fu, X. Gao, Y. Wang, D. Xu, C. Zhang, Z. Sun, Y. Lu, D. J. Young, H. Li, X.-C. Hang, *J*. *Phys*. *Chem*. *Lett*. **13**, 1494–1499 (2022).
[21] J. Yao, S.C. Dong, B. S. T. Tam, C. W. Tang, *ACS Appl*. *Mater*. *Interfaces* **15**, 7255–7262 (2023).
[22] W. Yuan, T. Huang, J. Zhou, M.-C. Tang, D. Zhang, L. Duan, *Nat*. *Commun*., **16**, 4446 (2025).
[23] M. Morgenroth, T. Lenzer, K. Oum, *J*. *Phys*. *Chem*. *C*, **127**, 4582-4593 (2023).
[24] J.-H. Lee, S.-H. Cheng, S.-J. Yoo, H. Shin, J.-H. Chang, C.-I. Wu, K.-T. Wong, J.-J. Kim, *Adv*. *Funct*. *Mate*., **25**, 361-366 (2015).
[25] Y. Tsuchiya, S. Diesing, F. Bencheikh, Y. Wada, P. L. d. Santos, H. Kaji, E. Z.-Colman, I. D. W. Samuel, C. Adachi, *J*. *Phys*. *Chem*. *A*, **125**, 8074–8089 (2021).
[26] M. Zhang, K. Wang, C.-J. Zheng, D.-Q. Wang, Y.-Z. Shi, H. Lin, S.-L. Tao, X. Li, X.-H. Zhang, *Front*. *Chem*., **7**, 16 (2019).
[27] K.-H. Kim, S.-J. Yoo, J.-J. Kim, *Chem*. *Mater*., **28**, 1936-1941 (2016).

View Article Online
DOI: 10.1039/D5TC04017E

Data Availability

The data supporting the findings of this study are available within the article and its Supporting Information. Additional raw data files are available from the corresponding author upon reasonable request.